Revealing the age of NGC 2509 with Gaia EDR3

Thinh Nguyen[1]

[1]Department of Astrophysics and Planetary Science, Villanova University, 800 E Lancaster Avenue, Villanova, PA, 19085, USA

November 2021

Abstract

The age of the open cluster NGC 2509 has been an ambiguous topic due to widely different values determined by different studies. With the recent significant improvement of *Gaia* Early Data Release 3, we aim to resolve the confusion by using the updated data to determine the cluster's age and other parameters such as modulus, metallicity, and absorption. We employ pyUPMASK, an unsupervised cluster algorithm, to calculate the membership probability and then select 254 cluster members whose membership probability is larger than 0.5. These stars are then used as input for the BASE-9 tool to find the best fitted stellar isochrone using the Markov chain Monte Carlo. After 50000 iterations, we obtain the estimated value of 9.2777 ± 0.00518, 0.2238 ± 0.01527, 11.635 ± 0.01109, and 0.0199 ± 0.00576 for logAge, [Fe/H], observed modulus, and absorption A_V, respectively. Our determined age is consistent with about half of the previous studies while disagrees with the others. The results of the metallicity and absorption are greatly different from the values in the literature. However, it should be noted that earlier studies assumed solar metallicity for this cluster.

A Introduction

In an open cluster, stars are born approximately at the same time and distance as well as composed of identical chemical compositions, mass is the determining variable that differs among the stars (von Hippel, 2005). Because more massive stars leave the main sequence earlier and open clusters have stars from a wide range of masses, the color-magnitude diagram (CMD) of open clusters usually has a distinct feature called the main-sequence turn-off point. Thus, one can fit an isochrone, a curve on the CMD representing a stellar population with similar age, to a star cluster to compute cluster parameters. Isochrones are calculated by using simulations to evolve an initial set of stars with the same composition to certain ages. Different theoretical isochrones are compared with the observational CMD to determine the best match.

Even though isochrone fitting is a good method to determine open cluster parameters, it has some drawbacks when the data is sparse or inaccurately defined. NGC 2509 is an example of such a case. NGC 2509 is an open cluster (Kharchenko et al., 2013) located approximately at $08^{\mathrm{h}}00^{\mathrm{m}}48^{\mathrm{s}}$ for right ascension (RA) and $-19°03'06''$ for declination (Dec). Recently, the distance to NGC 2509 is confirmed to be around 2500 parsec (Cantat-Gaudin et al., 2018) using *Gaia* Data Release 2 (DR2) (Gaia Collaboration et al., 2018). The cluster had been a topic of debate as different studies resulted in very different and confusing values for its age (Carraro & Costa, 2007; Sujatha & Babu,

2003). In particular, even though they all used the same method of isochrone fitting, Sujatha & Babu (2003) reported the age to be 8 billion years old, Ahumada (2000) computed it to be 1 billion, Kharchenko et al. (2013) shows that it is 1.6 billion, in Carraro & Costa (2007)'s work it is 1.2 billion, and in the most recent paper, de Juan Ovelar et al. (2020) estimated it to be 861 million years old. This discrepancy might be explained by the different data used to plot the CMD: Cantat-Gaudin et al. (2018) and de Juan Ovelar et al. (2020) used *Gaia* DR2 data while Sujatha & Babu (2003) and Ahumada (2000) used CCD photometry of their telescopes. Also, different isochrone models or fitting methods can also be a cause. For example, Sujatha & Babu (2003) uses the old zero age main sequence model by Landolt-Bornstein (1982), or de Juan Ovelar et al. (2020) fits the isochrone by visual inspection. Furthermore, unlike other open clusters, NGC 2509 has a quite narrow main sequence turn off (de Juan Ovelar et al., 2020) and does not contain a lot of stars in that region, which brings greater challenges in fitting the correct isochrone to the cluster's morphology in the CMD.

With the recent publication of *Gaia* Early Data Release 3 (EDR3), we propose to use the new data to verify and re-determine the age and other parameters of NGC 2509. *Gaia* (Gaia Collaboration et al., 2016) is a space mission by the European Space Agency (ESA) that surveys all astrometric, photometric, and spectroscopic measurements of our Galaxy on an all-sky scale on only one platform. The precision in *Gaia*'s astrometry is unprecedented with the accuracy down to 24 microarcseconds (Gaia Collaboration et al., 2016). Compared to *Gaia* DR2, *Gaia* EDR3 demonstrates a significant improvement in many aspects. Specifically, precision increases by 30% in parallax measurements and by 200% in proper motions (Gaia Collaboration et al., 2021). There are also better photometric measurements and a greater homogeneity across color, magnitude, and coordinate (Gaia Collaboration et al., 2021). Thus, as previous studies on the cluster were conducted with DR2 data, all of these improved elements of EDR3 are crucial to explore the confusion around NGC 2509.

The project employ robust techniques in the field of open clusters to ensure the best possible result. These include the Bayesian approach proposed by Sampedro & Alfaro (2016) to determine the cluster membership and the open-source software Bayesian Analysis for Stellar Evolution with Nine Variables (BASE-9) (von Hippel et al., 2006) to compute the cluster's parameters (age, metallicity, line-of-sight absorption, and distance modulus) by isochrone fitting. The details of these techniques will be further discussed later in the paper. Combined with improved data that minimize the interfering scattering effect, the techniques will help further refine the cluster's parameters.

The paper will be structured as follows. Section B elaborates the methods that are utilized for cluster membership calculation and isochrone fitting. The results of the computations are discussed and compared with literature in Section C. Lastly, Section D summarizes all the analysis and explains the further implication.

B Methodology

B.1 Data

The study utilizes photometry (G, BP, and RP mean magnitude) astrometry (parallax and proper motions) data from *Gaia* EDR3 public archive [1]. The query was conducted with a 14 arcmin radius search around the NGC 2509's coordinate ($08^{\mathrm{h}}00^{\mathrm{m}}48^{\mathrm{s}}$, $-19°03'06''$). Sánchez et al. (2020) calculate the radius of NGC 2509 to be 8.15 arcmins from *Gaia* DR2 data. Therefore, we overestimated the searched radius to be 14 arcmins to include all possible cluster members. As a result, the query

[1] https://gea.esac.esa.int/archive/

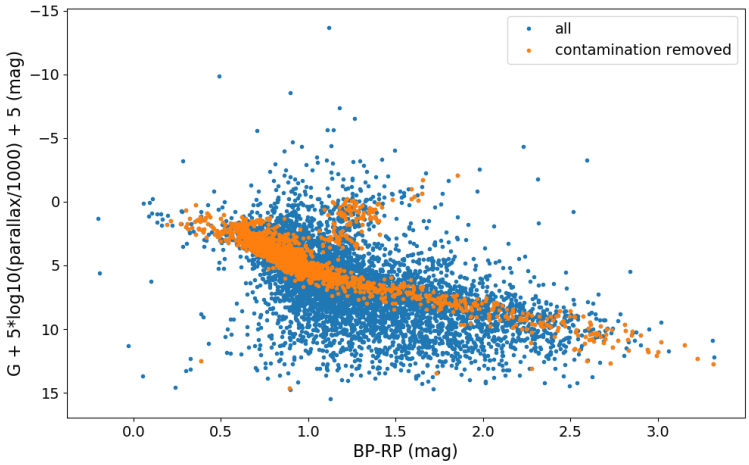

Figure 1: The color-absolute magnitude diagram of NGC 2509 from the *Gaia*'s query and after the contamination removal procedure described in Equation 1.

returns 10260 targets.

B.2 Contamination removal

After obtaining the query result, we first remove targets without data on either photometry, proper motion, or parallax. Next, because calculating the cluster membership probability relies heavily on the astrometric information, to receive the best possible cluster members, we limit contaminated and unreliable sources by applying some restrictions on the *Gaia*'s astrometric parameters, specifically

$$\begin{aligned} &\texttt{ruwe} \leq 1.4 \\ &\texttt{astrometric\_excess\_noise\_sig} \leq 2 \\ &\texttt{parallax\_over\_error} \geq 5. \end{aligned} \tag{1}$$

In the criteria, `ruwe` stands for the renormalized unit weight error. Sources that a have good fit to a single-star model are expected to have the `ruwe` value approximate to 1. A large `ruwe` indicates that the examined sources are not single stars or there are problems with their astrometric solution (Lindegren et al., 2021; Lindegren, 2018). We take the recommended value by *Gaia* of 1.4 (Lindegren, 2018) for `ruwe`. While this limit can accidentally remove some binary stars, we want to take a conservative approach and ensure the best astrometric solution as possible for the isochrone fit. Regarding the second part of the restriction, the `astrometric_excess_noise` measures the inconsistency between observations and the best fitting standard astrometric models. The value is considered significant if the `astrometric_excess_noise_sig` is larger than 2. Therefore, we set the limit at 2 to obtain astrometrically reliable sources (Lindegren et al., 2021). Finally, we require the parallax measurement to be at least five times larger than its uncertainty to ensure only good photometric solutions. As a result, from 10260 targets in the query, we narrow down our sample to 1683 targets with reliable astrometric solutions. Figure 1 displays the color - absolute magnitude diagram of our sample before and after the contamination removal procedure.

Table 1: The membership probability and the cross-match to *Gaia* DR2 data (Cantat-Gaudin et al., 2018) of our 1683 targets after the contamination removal. The full table will be provided in the online version of this paper.

source_id	ra	dec	parallax	G_mag	memprob	GaiaDR2_list
5714593006829895296	120.401	-18.973	0.81839	18.38082	0	FALSE
5714593011132883712	120.392	-18.978	0.2699	14.89579	0	FALSE
5714593247348100096	120.393	-18.961	0.393944	15.5026	0.0031	FALSE
5714593286010564480	120.382	-18.960	0.186318	13.87069	0	FALSE
5714402417663936512	120.044	-18.985	0.345859	16.30059	0.9994	TRUE

B.3 Membership probability

To determine the cluster membership probability, we utilize pyUPMASK, an unsupervised cluster algorithm (Pera et al., 2021). pyUPMASK is an enhanced and faster version of UPMASK (Krone-Martins & Moitinho, 2014) and also converts the UPMASK's original code in R language to Python language. Both UPMASK and pyUPMASK share a similar 2-loop procedure to assign cluster membership probability. Initially, using the non-positional features (in our case, we use proper motions), the clustering method is responsible for dividing the whole cluster data into smaller clusters with N members per cluster. In the inner loop, for each sub-cluster, the random field rejection method is applied to test for clumps in positional space. The method will compare the kernel density estimation of the coordinate space to that of a two-dimensional uniform distribution in the same range. If the two kernels are adequately similar, all stars in that sub-cluster can be viewed as randomly distributed. Therefore, they are considered as field stars and will be rejected; otherwise, they will be retained to another iteration of the inner loop. The inner loop ends when no more stars are dismissed. Next, the outer loop will randomly divide the original cluster again to feed the inner loop, and the whole cycle keeps repeating by the number of outer loops specified by the user. The membership probability for each star will be calculated by averaging the number of times that star is classified as a cluster member in each outer loop. For our use, we follow the pyUPMASK's default setting: mini-batch k-means for the clustering method (Sculley, 2010), 25 outer loops, 25 maximum inner loops, and 25 members per sub-cluster.

Once having all stars' membership probability, we decided to set a cut-off value of 0.5 for a cluster member. As a result, we have 254 cluster member stars and 1429 field stars in our sample. Detailed membership probability will be provided in a table along with the online version of this paper and Table 1 is a small version of that table. In Figure 2, the color-apparent magnitude diagram of our cluster shows a clear main-sequence with its turnoff point. We can also discern red giants and a binary sequence that is parallel to the main sequence. While we do not have any white dwarfs or blue stragglers in our sample, the absence of those stars do not significantly affect our isochrone fitting as long as the turn-off point is visible.

B.4 Fitting isochrone

Having the NGC 2509's list of members, we adopt the open-source software Bayesian Analysis for Stellar Evolution with Nine Variables (BASE-9) (von Hippel et al., 2006) to determine the cluster's parameters. This method uses the Bayesian approach to fit a set of theoretical isochrones with the observational distribution of cluster members. Particularly, in our use, we employ the stellar evolution track model PARSEC (Bressan et al., 2012) because it provides isochrones with *Gaia* photometric filters. BASE-9 adjusts its set of parameters for each iteration by using the Markov

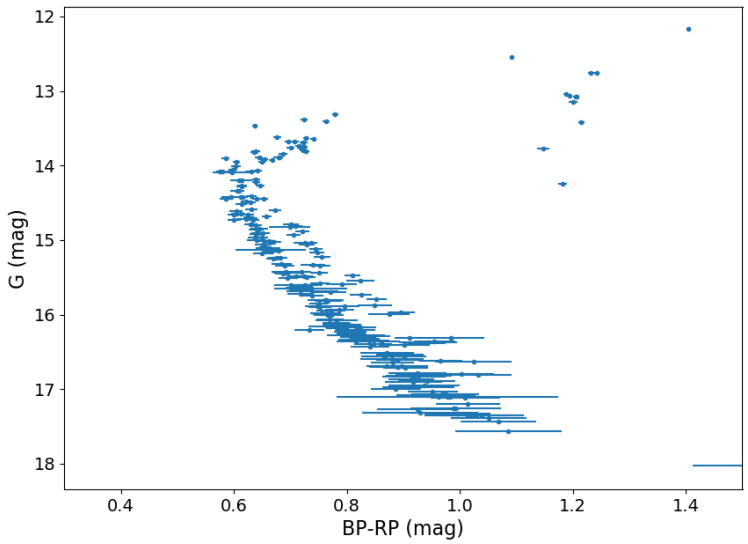

Figure 2: The color-apparent magnitude diagram of 254 NGC 2509's member stars, which are identified by pyUPMASK with the membership probability larger than 0.5

chain Monte Carlo (MCMC) technique. MCMC involves random sampling from the probability distribution to estimate a set of quantities, in which one sample step is dependent on the previous step. The probability for each set of parameters is determined by how close its fit is to the data points. In the parameter space, the sampling process will tend to focus on regions with high probability and will be less likely to move into regions with low probability. After a certain iteration, when the MCMC's convergence is achieved, we can estimate the desired quantities with the posterior distributions.

Among the list of parameters available in BASE-9, we aim to estimate the cluster's logAge, metallicity ([Fe/H]), the extinction in V band (A_V), and observed modulus, which accounts for both distance and extinction. We leave helium mass fraction and carbonicity for white dwarfs fixed at the BASE-9's default values of 0.29 and 0.38, respectively. We set our prior mean for the logAge and absorption A_V, to be 9.08 and 0.322, which come from Carraro & Costa (2007) and Kharchenko et al. (2013), respectively.

Regarding the prior observed modulus, because we do not not know the absorption coefficient yet, we will use the intrinsic modulus as an estimated prior. The intrinsic modulus and its standard deviation can be computed by

$$\begin{aligned} (m-M)_0 &= -5 \times \log10(\varpi) - 5, \\ \sigma_{(m-M)_0} &= \frac{-5}{\ln(10)} \times \frac{\sigma_\varpi}{\varpi}, \end{aligned} \tag{2}$$

in which ϖ and σ_ϖ are the weighted mean and the corresponding standard deviation of the *Gaia* parallax distribution of the cluster members, as shown in Figure 3. The weight in the average calculation is the `parallax_error` parameter provided by *Gaia*. With the parallax mean of 0.376 mas and parallax standard deviation of 0.045 mas, the prior mean and sigma for modulus are 12.124 and 0.26, respectively. Also, the reason why we do not use these values to compute distance directly is that the *Gaia* astrometric solution often overestimates the actual distance, and thus the distance

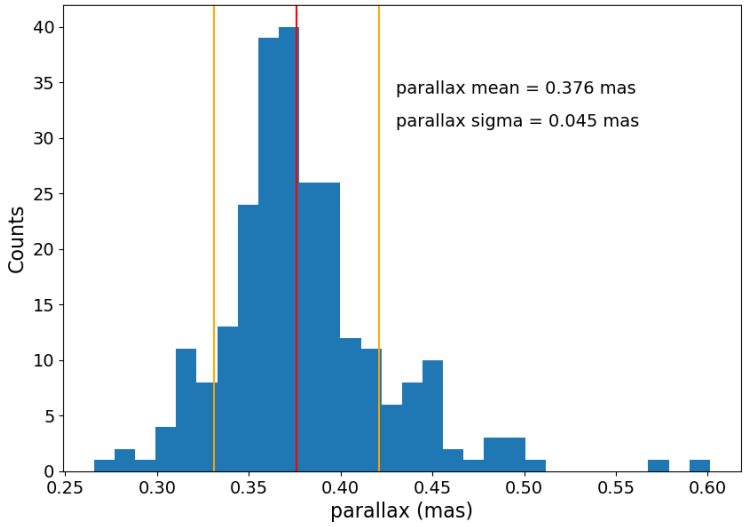

Figure 3: The parallax distribution of 254 member stars. The weighted mean (red line) and the standard deviation (orange lines) of the distribution are used to calculate the prior mean and sigma for modulus in the BASE-9 MCMC run.

obtained through Bayesian inference is more preferable (Luri et al., 2018).

Since we do not have any information regarding the metallicity, we leave the prior mean as the default value of 0.0 and set its prior sigma to be 0.1. This value is a reasonable assumption as the metallicity of open clusters often falls in the range of -0.3 to 0.3 (Netopil et al., 2016). We also want to note that we chose the sigma for logAge to be uniform, as we want the age to be free to vary throughout the parameter space. Besides the four examined parameters, we fix the other two - helium mass fraction and carbonicity for white dwarfs - at the default values of 0.29 and 0.38, respectively. The number of iteration used in our run is 50000. For the step sizes, we left the default values of 0.005, 0.005, 0.005, 0.002 for the logAge, [Fe/H], modulus, and A_V, respectively. However, for other runs in the robustness analysis described in Section C.3, we chose larger step sizes for the priors that are further from the posterior results so that the code can move through the parameter space faster. It is important to note that our chosen step sizes are all smaller or equal to their corresponding prior sigma, and the step sizes only affect the efficiency of the MCMC run but not the posterior results. The summary of all the prior parameters can be found in Table 2.

To test for convergence after 50000 iterations in our MCMC run, we employ the diagnostic plot showing the log of the posterior probability as a function of iteration. According to Figure 4, there is not upward or downward trend in the plot and the posterior probability stays relatively uniform. Thus, the plot helps qualify convergence and therefore we can start analyzing the posterior distributions.

The average posterior parameters are determined by calculating the weighted mean for each posterior distribution obtained from BASE-9. The weight is the negative log of the unnormalized posterior probability (or $-$logPost, in which logPost is the value provided by BASE-9). We chose the weight as such because the absolute value of logPost is proportional to Chi-square, a value that determines how close the fit is to the observed data. Therefore, the MCMC runs with a larger absolute value of logPost are weighted more significant. These posterior distributions only come from the 50000 iterations of the MCMC's adaptive run, and we do not take into account values

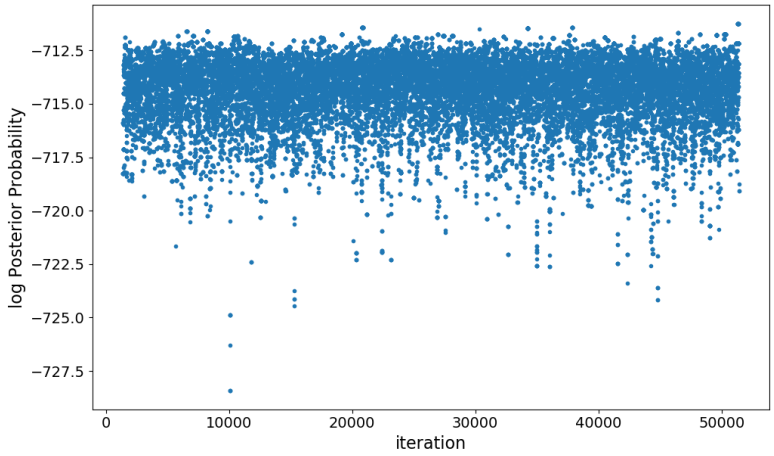

Figure 4: The log of unnormalized posterrior probability as a function of iteration to test for convergence. There is no upward or downward trends in the plot, suggesting that the run has reached convergence.

Table 2: The BASE-9 prior and posterior parameters of NGC 2509's logAge, metallicity [Fe/H], observed modulus, extinction A_V, helium mass fraction, and carbonicity. The helium mass fraction and carbonicity are fixed during the MCMC run.

	Prior mean	Prior σ	Step size	Posterior mean	Posterior σ
logAge	9.08	uniform	0.005	9.2777	0.00518
[Fe/H]	0.0	0.1	0.005	0.2238	0.01527
modulus	12.124	0.26	0.005	11.635	0.01109
A_V	0.322	0.1	0.002	0.0199	0.00576
He mass fraction	0.29	0.0	0.0	0.29	0.0
Carbonicity	0.38	0.0	0.0	0.38	0.0

from the initial burnin stages.[2] The weighted mean and its corresponding standard deviation of each parameter is given in Table 2.

All the mean posterior parameters are utilized with the module `makeCMD` in BASE-9 to compute the average isochrone that fits the color-apparent magnitude diagram of the cluster. Figure 5 demonstrates the fitted isochrone goes through most of the data points. Even though there are few red giants, the isochrone still fits well with the turnoff point and the red giant branch.

C Discussion

C.1 Membership comparisons with literature

We compare our list of members from using *Gaia* EDR3 data with that from using *Gaia* DR2 data (Cantat-Gaudin et al., 2018) to detect similarities between the two *Gaia* data releases. Similar to us, Cantat-Gaudin et al. (2018) used the UPMASK method (Krone-Martins & Moitinho, 2014) to

[2]The intial samples that allow MCMC to move from the starting point to the equilibrium distribution. As set by the BASE-9's default, there is a maximum of 2000 iterations during burn-in stages.

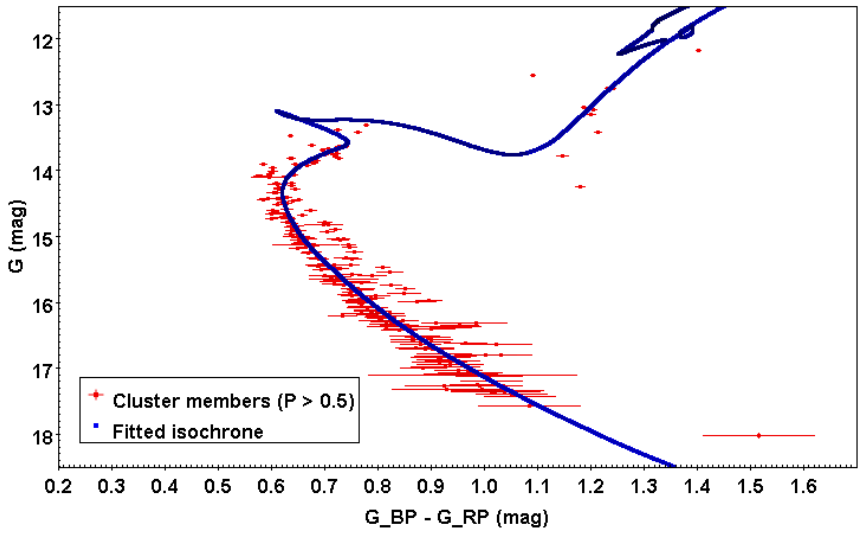

Figure 5: The fitted isochrone with parameters listed in Table 2 is over-plotted on the NGC 2509's member stars.

detect 253 NGC 2509's members whose membership probability is larger than 0.5. For us, that number is 254, as discussed in Section B.3. We perform the cross-match by comparing the EDR3 coordinates (RA and DEC) in our list with their DR2 coordinates. Given the maximum separations between 2 matched points of 1 arcsec, we obtain 203 overlapped targets (80% of our list). This high percentage emphasizes the consistency between our work and the literature and between the two *Gaia*'s data releases. The list of the cross-matched targets will be provided in the membership probability table along with the online version of this table. A short version of the table can be viewed in Table 1.

C.2 Corner plot

To study the correlation between the samplings in the 4-parameter space, we produce the corner plot by employing the Python module `corner.py` (Foreman-Mackey, 2016). The visualization plots the two-dimensional projection of the MCMC samplings from BASE-9 to reveal possible covariances and to test the samplings' convergence. In our corner plot displayed in Figure 6, all posterior distributions look Gaussian, which is another indication that MCMC has reached convergence with the iteration number of 50000. The contour plots signify the combination that has the same Chi-square value between the fit and the data points (i.e, any combinations along one contour line will result in a fit with similar significance in regards to the data points and therefore one combination is not preferable than the other). In the first column, the contour plots show two peak density regions, suggesting that the distribution of logAge is bi-modal. Moreover, the elliptical shape of some contour plots demonstrates that there are correlations between parameters. Specifically, a strong negative correlation exists between [Fe/H] and logAge, modulus and logAge, and [Fe/H] and absorption. On the other hand, a moderate positive correlation appears between [Fe/H] and modulus. It is important to note that these correlations are specific to this MCMC run and do not represent the characteristics of open clusters in general. Taken the relationship between logAge and modulus as an example, during the MCMC run, when the walker increases the logAge, the modulus needs to be decreased to get a good fit to the data point. This does not mean that logAge is inversely proportional to modulus in a general context. Lastly, the concentric pattern in

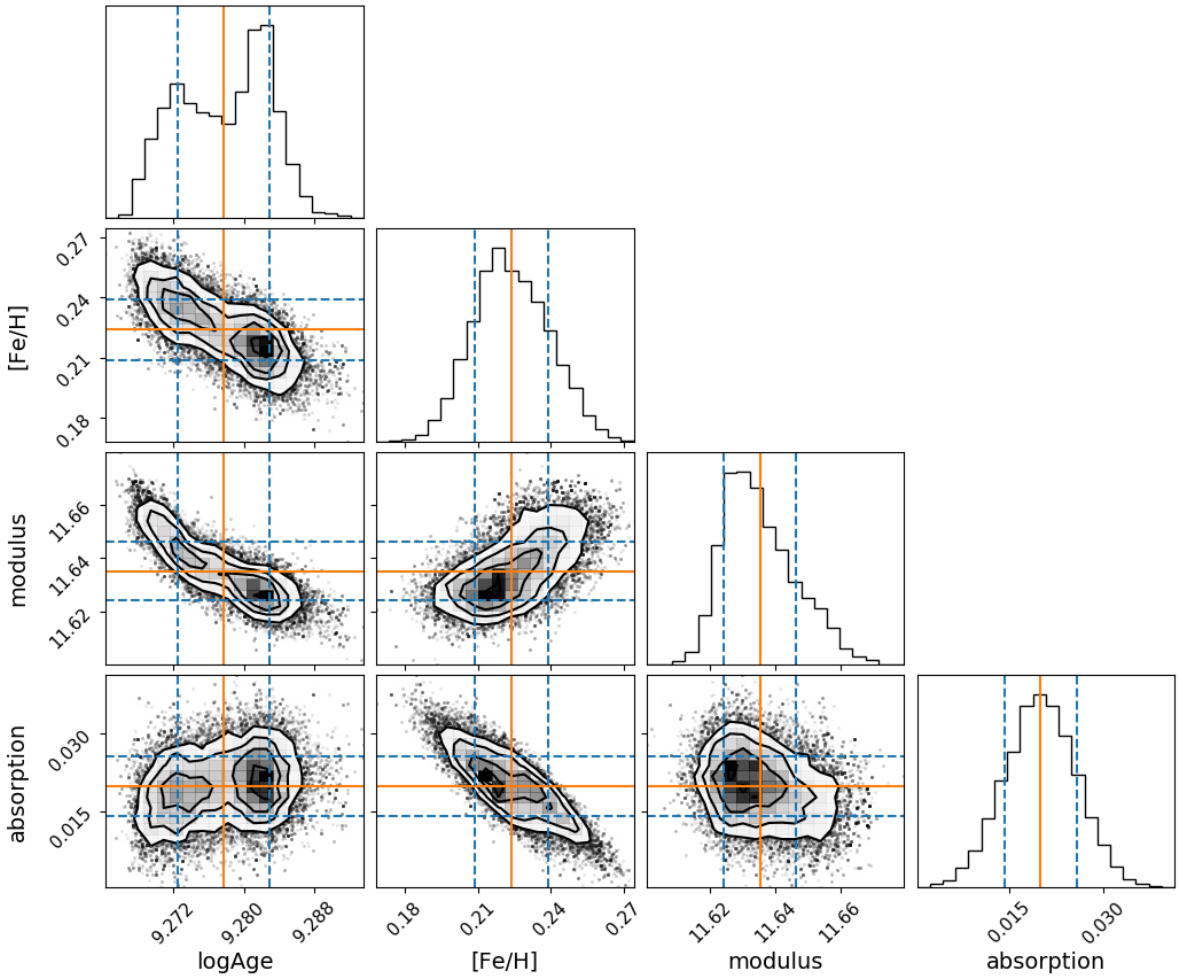

Figure 6: The corner plot showing the posterior distributions and their correlations. All posterior distributions look Gaussian or a combination of Gaussian distributions, which is another indication that MCMC has reached convergence. Correlations between [Fe/H]-logAge, [Fe/H]-modulus, [Fe/H]-absorption, and modulus-logAge are noticeable in the plot.

the absorption-modulus and the absorption-logAge contour plots infers that there is no relations between the two variables during the MCMC runs. The corner plot also helps us evaluate the accuracy of our average posterior parameters. In the plot, the orange lines represent the weighted means of the posterior parameters (as given in Table 2). Two blue dashed lines show one standard deviation around the weighted mean. As all intersections among the orange lines are located at the highest density region ad within the 1-σ regions of the contour plots, we are more confident with our results for NGC 2509.

C.3 Robustness analysis

Another method to evaluate the convergence of the MCMC run is to do the robustness analysis with different starting priors. In robustness analysis, we tried different sets of prior values to see their effect on the posterior distributions. Beside the set of prior values described in Section B.4, we

Table 3: The robustness analysis of the Bayesian approach of BASE-9. We examine the effect of the prior on the posterior by using 3 different logAge values and 2 different absorption values (6 combinations in total).

Prior				Posterior			
logAge	FeH	m-M	A_V	logAge	FeH	m-M	A_V
9.08	0.0	12.124	0.322	9.2777 ± 5.2e-3	0.2238 ± 1.5e-2	11.635 ± 1.1e-2	0.0199 ± 5.8e-3
9.2	0.0	12.124	0.322	9.2774 ± 5.3e-3	0.2241 ± 1.6e-2	11.636 ± 1.2e-2	0.0200 ± 5.9e-3
9.9	0.0	12.124	0.322	9.2772 ± 5.1e-3	0.2254 ± 1.6e-2	11.636 ± 1.1e-2	0.0196 ± 5.9e-3
9.08	0.0	12.124	0.465	9.2782 ± 5.1e-3	0.2226 ± 1.5e-2	11.635 ± 1.1e-2	0.0201 ± 5.6e-3
9.2	0.0	12.124	0.465	9.2777 ± 5.1e-3	0.2227 ± 1.5e-2	11.635 ± 1.1e-2	0.0206 ± 6.1e-3
9.9	0.0	12.124	0.465	9.2777 ± 5.2e-3	0.2236 ± 1.5e-2	11.635 ± 1.1e-2	0.0201 ± 5.9e-3

use two other logAge values of 9.2 and 9.9 Kharchenko et al. (2013); Dias et al. (2002) and another absorption value of 0.456 from Dias et al. (2002), resulting in an addition of five more prior sets. Other configuration parameters such as step size and prior σ are kept the same as in Section B.4. Table 3 shows the MCMC results for these four sets. According to the table, the different prior values ineligibly affect the posterior parameters. For example, at the prior absorption of 0.465, when we change our prior logAge from 9.2 to 9.9 (0.7 unit difference), the posterior logAge remains identical to the fourth decimal place. Similarly, at the prior logAge of 9.08, the change of 0.143 in the prior absorption value (from 0.456 to 0.322) only returns the changes of 0.0002 in the posterior absorption value (from 0.0199 to 0.0201). Furthermore, the posterior [Fe/H] and modulus do not significantly alter among the six prior sets. This similarity is another sign showing that all our MCMC runs have reached convergence.

The robustness analysis also strengthens our results among the debate around NGC 2509's age. As pointed out in Section A, regarding the cluster's age, some possible values in the debate are around 8 billion years old (logAge of 9.9) (Sujatha & Babu, 2003; Dias et al., 2002), around 1 billion years old (logAge of around 9.0) (Carraro & Costa, 2007; Ahumada, 2000), and around 1.6 billion years old (Kharchenko et al., 2013). When we put all these possible values as priors, they all return the posterior age of 1.895 billion years old (logAge of 9.2777). Therefore, given the accuracy of *Gaia* EDR3 data and the model, our value remains consistent among different prior ages that are discussed in the literature.

C.4 A note on metallicity and absorption

Among the four parameters, the posterior logAge and modulus do not shift much from the prior values, while the posterior metallicity [Fe/H] and the absorption A_V change significantly. Even though they are possible, the two posterior values of [Fe/H] and A_V are surprising. We found that NGC 2509 is relatively metal heavy ([Fe/H] = 0.2238) even though it is a young open cluster. However, this is still viable because previous studies did not provide metallicity or assumed solar metallicity when fitting isochrone (Dias et al., 2002; Kharchenko et al., 2013). Thus, we have not reference to compare our result. Also, the absorption value is small compared to the great distance that the cluster is at. However, the result of the robustness analysis confirms that these values of metallicity and absorption are unique to this data set. Therefore, additional works can try fixing the metallicity or absorption in the MCMC runs to see what effect it may have on the posterior distributions.

D Conclusion

In this study, we use *Gaia* EDR3 data to explore the logAge, metallicity [Fe/H], modulus, and absorption A_V of the open cluster NGC 2509. Our calculation using pyUPMASK algorithm (Pera et al., 2021; Krone-Martins & Moitinho, 2014) results in 254 stars whose membership probability is larger than 0.5, which is our criterion to declare a cluster member. The color-apparent magnitude diagram of the cluster members shows a clear main sequence with a noticeable turn-off point. The result of BASE-9 (von Hippel et al., 2006), a method to fit isochrone by using Bayesian analysis with MCMC, are 9.2777 ± 0.00518, 0.2238 ± 0.01527, 11.635 ± 0.01109, and 0.0199 ± 0.00576 for logAge, [Fe/H], modulus, and A_V, respectively. We also show that the test reached convergence by examining the corner plot and conducting the robustness analysis with different sets of priors.

In response to the confusion around the age of NGC 2509, we found the age of NGC 2509 to be approximately 1.9 billion years. This value is relatively consistent with the values of Ahumada (2000); Carraro & Costa (2007); Kharchenko et al. (2013), but is different from the values of de Juan Ovelar et al. (2020) and especially the value of 8 billion years old by Sujatha & Babu (2003); Dias et al. (2002). We also found that the posterior values for [Fe/H] and A_V are somewhat surprising. Thus,instead of having them vary freely right now, additional work to fix these two parameters while running BASE-9 is needed.

E Acknowledgement

We would like to thank Dr. Andrej Prsa, Dr. Scott Engle, Dr. von Hippel, and Dr. Laurent Eyer for the valuable help and discussion while doing this project. Notably, this study relies heavily on using BASE-9, and Dr. von Hippel helps us learn to use the code much faster.

F Bibliography

Ahumada, J. A. 2000, in Astronomical Society of the Pacific Conference Series, Vol. 198, Stellar Clusters and Associations: Convection, Rotation, and Dynamos, ed. R. Pallavicini, G. Micela, & S. Sciortino, 43

Bressan, A., Marigo, P., Girardi, L., et al. 2012, MNRAS, 427, 127, doi: 10.1111/j.1365-2966.2012.21948.x

Cantat-Gaudin, T., Jordi, C., Vallenari, A., et al. 2018, A&A, 618, A93, doi: 10.1051/0004-6361/201833476

Carraro, G., & Costa, E. 2007, A&A, 464, 573, doi: 10.1051/0004-6361:20066350

de Juan Ovelar, M., Gossage, S., Kamann, S., et al. 2020, MNRAS, 491, 2129, doi: 10.1093/mnras/stz3128

Dias, W. S., Alessi, B. S., Moitinho, A., & Lépine, J. R. D. 2002, A&A, 389, 871, doi: 10.1051/0004-6361:20020668

Foreman-Mackey, D. 2016, The Journal of Open Source Software, 1, 24, doi: 10.21105/joss.00024

Gaia Collaboration, Prusti, T., de Bruijne, J. H. J., et al. 2016, A&A, 595, A1, doi: 10.1051/0004-6361/201629272

Gaia Collaboration, Brown, A. G. A., Vallenari, A., et al. 2018, A&A, 616, A1, doi: 10.1051/0004-6361/201833051

—. 2021, A&A, 649, A1, doi: 10.1051/0004-6361/202039657

Kharchenko, N. V., Piskunov, A. E., Schilbach, E., Röser, S., & Scholz, R. D. 2013, A&A, 558, A53, doi: 10.1051/0004-6361/201322302

Krone-Martins, A., & Moitinho, A. 2014, A&A, 561, A57, doi: 10.1051/0004-6361/201321143

Landolt-Bornstein. 1982, Landolt-Börnstein: Numerical Data and Functional Relationships in Science and Technology - New Series " Gruppe/Group 6 Astronomy and Astrophysics " Volume 2 Schaifers/Voigt: Astronomy and Astrophysics / Astronomie und Astrophysik " Stars and Star Clusters / Sterne und Sternhaufen, Vol. 2

Lindegren, L. 2018. http://www.rssd.esa.int/doc_fetch.php?id=3757412

Lindegren, L., Klioner, S. A., Hernández, J., et al. 2021, A&A, 649, A2, doi: 10.1051/0004-6361/202039709

Luri, X., Brown, A. G. A., Sarro, L. M., et al. 2018, A&A, 616, A9, doi: 10.1051/0004-6361/201832964

Netopil, M., Paunzen, E., Heiter, U., & Soubiran, C. 2016, A&A, 585, A150, doi: 10.1051/0004-6361/201526370

Pera, M. S., Perren, G. I., Moitinho, A., Navone, H. D., & Vazquez, R. A. 2021, A&A, 650, A109, doi: 10.1051/0004-6361/202040252

Sampedro, L., & Alfaro, E. J. 2016, MNRAS, 457, 3949, doi: 10.1093/mnras/stw243

Sánchez, N., Alfaro, E. J., & López-Martínez, F. 2020, MNRAS, 495, 2882, doi: 10.1093/mnras/staa1359

Sculley, D. 2010, in Proceedings of the 19th International Conference on World Wide Web, WWW '10 (New York, NY, USA: Association for Computing Machinery), 1177–1178, doi: 10.1145/1772690.1772862

Sujatha, S., & Babu, G. S. D. 2003, Bulletin of the Astronomical Society of India, 31, 9

von Hippel, T. 2005, arXiv e-prints, astro

von Hippel, T., Jefferys, W. H., Scott, J., et al. 2006, ApJ, 645, 1436, doi: 10.1086/504369